Hindawi
Journal of Nanomaterials
Volume 2020, Article ID 9346423, 8 pages
https://doi.org/10.1155/2020/9346423

Research Article

Jurkat T Cell Detectability and Toxicity Evaluation of Low-Temperature Synthesized Cadmium Quantum Dots

Ngoc Thuy Vo,[1,2] **Thi Bich Vu**,[3,4] **Hong Tran Thi Diep**,[1,2] **Thien Le Khanh**,[1,2] **Hieu Tran Van**,[1,2] **Thanh Binh Nguyen**,[4] **and Quang Vinh Lam**[1,2]

[1]*University of Science, Ho Chi Minh City 72711, Vietnam*
[2]*Vietnam National University, Ho Chi Minh City 71308, Vietnam*
[3]*Institute of Theoretical and Applied Research, Duy Tan University, Ha Noi 100000, Vietnam*
[4]*Institute of Physics, Vietnam Academy of Science and Technology, 10 Dao Tan, Ba Dinh, Ha Noi, Vietnam*

Correspondence should be addressed to Ngoc Thuy Vo; vtnthuy@hcmus.edu.vn

Received 15 April 2020; Accepted 19 May 2020; Published 12 June 2020

Guest Editor: Xiao Jin

Early and highly accurate detection of diverse diseases is in urgent demand than ever, especially for cancers and infectious ones. Among possibilities, biosensing by utilizing conjugated nanoparticles is still a method of choice. However, the toxicity of quantum dots remains a big matter of concern in those biooriented applications. In this study, mercaptosuccinic acid-coated cadmium selenide quantum dots of approximately 2.3 nm were synthesized with a simple green method at low temperature and cost-saving chemicals. The influence of synthesis factors was investigated with different spectroscopic methods. The toxicity issue was evaluated on the NIH-3T3 cell line (ATCC® CRL-1658™) and an MTT assay, revealing a secure threshold of 20 μg/ml. Consequently, successful conjugation to the CD3 antibody including an A/G protein bridge was implemented and verified with fluorescent methods. Finally, Jurkat T cell detectability of conjugated CdSe was successfully validated with fluorescent microscopy. The CdSe-based products are accessible for future biosensing applications.

1. Introduction

For years, understanding of semiconducting quantum dots along with their unique properties of zero-dimensional structure has been extensively accumulated not only through diverse synthesis methods but also through novel applications [1–5]. Thanks to the primary advantages such as high stability, broad photoluminescence and absorption spectra, large Stoke shift, long lifetime, and an order of luminescent intensity higher than organic dyes and fluorescent protein counterparts [6, 7], quantum dots have been employed widely in biology especially in biomarking and biosensing [8–10].

A huge effort has been paid out on the fabrication and characterization of highly luminescent quantum dots derived from trioctylphosphine oxide- (TOPO-) or trioctylphosphine- (TOP-) mediated routes of high temperatures and costly chemicals. However, such quantum dots exhibited low dispersion in water and an inability to be directly applied in biology without surface functionalization [11–13]. Recent reports have focused on fabricating highly stable CdSe quantum dots in water with surfactants comprising thiol groups [14–17]. These nanoparticles could be applied straightly into bioapplications on the one hand, but low luminescence intensity due to dislocation or surface defects was a big drawback. Till now, novel synthesis methods have continuously been introduced to achieve nanoparticles of high quality and high luminescence as well as time and cost saving [18]. Following the trend, this work was aimed at synthesizing mercaptosuccinic acid- (MSA-) coated quantum dots of high quality, high luminescence, and high biocompatibility from inexpensive chemicals without metal-organic precursors. Effects of temperature, reaction time, and pH values on optical properties and structure were under investigation with UV-visible absorption, photoluminescence (PL), Fourier transform infrared spectroscopy, X-ray diffraction (XRD), and transmission electron microscopy (TEM). Experimentally, quantum

dots cause a greater effect of toxicity compared to bulky counterparts at the same mass dose [19–21]. Potential toxicity and hazardous adverse effects of bare CdSe quantum dots on biological samples have always posed a concern much greater than the core/shell CdSe/ZnS counterparts. In practice, toxicity evaluation of CdSe without a protective shell layer is a crucial step toward basic knowledge and further bioapplications. We evaluated the quantum dot toxicity by using the NIH-3T3 cell line (ATCC® CRL-1658™) and an MTT assay to determine a nontoxic threshold of high cell viability. A cadmium selenide quantum dot concentration of 20 μg/ml was found to be the safe level from which cells presented a great chance for survival (97.4% on average). Finally, for the detection of Jurkat T cells, conjugation of the CD3 antibody to MSA-capped CdSe quantum dots was implemented. In this process, the A/G protein played a role as a vital connector to enhance CD3 antibody-CdSe quantum dot association. Successful conjugation of the A/G protein and the CD3 antibody was verified with photoluminescence and time-resolved fluorescence characterizations. The final products are eminently promising and relevant to further development.

2. Experiment

2.1. Synthesis of MSA-Coated CdSe Quantum Dots. All chemicals in MSA-capped CdSe quantum dot synthesis were of analytical grade and brought into use without further purification: mercaptosuccinic acid (MSA), cadmium acetate dehydrate ($Cd(CH_3CO_2)_2{\cdot}2H_2O$), sodium selenite pentahydrate ($Na_2SeO_3{\cdot}5H_2O$), sodium borohydride ($NaBH_4$), sodium hydroxide (NaOH, 99%), methanol, toluene, and phosphate buffer saline solution (PBS, pH 7.0).

Initially, 1.53 mmol of $Cd(CH_3CO_2)_2{\cdot}2H_2O$, 1.85 mmol of MSA, and 50 ml of distilled water were added into a three-neck flask to produce a Cd^{2+} precursor. The mixture was stirred in a nitrogen atmosphere until MSA was completely dissolved. Nitrogen gas was introduced to eliminate oxygen and the resulting acetic acid. To adjust pH, NaOH was gradually dropped to reach the expected value (6.0-11.5). For the Se^{2-} precursor, 2.64 mmol of $NaBH_4$, 1.34 mmol of $Na_2SeO_3{\cdot}5H_2O$, and 5 ml of water were mixed up for 15 minutes. We rapidly injected the Se^{2-} precursor into the Cd^{2+} solution at room temperature. The mixture was then stirred for 30 minutes at 600 rpm. The solution was then heated up to three different reaction temperatures (90°, 95°, or 100°C) without stirring. After some time, toluene was injected to rapidly cool down the solution and to intentionally stop the development of particles. The as-synthesized products were finally dispersed in PBS 7.0 buffer solution for long-time preservation. A simple method of preparation, common chemicals, and reasonably low synthesis temperature are the three big advantages of this method.

2.2. Toxicity Evaluation of Quantum Dots. The toxicity of quantum dots was analyzed using the NIH-3T3 cell line (ATCC® CRL-1658™) and the MTT assay. NIH-3T3 cells were grown in DMEM-10 medium (HiMedia) supplemented with 10% fetal bovine serum (FBS) and antibiotics (Sigma). Cells were seeded onto a 96-well plate (5×10^3 cells per well) in 100 μl DMEM-10 and incubated at 37°C in 5% CO_2 for 24 hours. After this time, cells were washed, supplemented with 100 μl of DMEM-10 containing quantum dots with different concentrations of 2×10^3, 2×10^2, 2×10^1, and 2×10^0 μg/ml, and incubated at 37°C in 5% CO_2 for 48 hours. Then, 5 μg/ml of MTT (Sigma) was added at a ratio 1/10 (v/v), cells were incubated for 3 hours, and optical density (OD) was measured at a wavelength of 550 nm (Multiskan Ascent). The results were normalized to respective control samples.

2.3. CD3 Antibody Conjugation to Quantum Dots. For conjugation of the CD3 antibody to MSA-capped CdSe quantum dots, the A/G protein was employed as an essential bridge to firmly enhance antibody-quantum dot connection efficiency. For this reason, a higher antibody-antigen interaction performance could be achieved later. Initially, acid-coated quantum dots were shaken in 5% BSA at 10°C for two hours to ensure that there was no direct interaction between quantum dots and cells through nonspecific bonds. Consequently, we supplied antibodies to Jurkat T cells [10, 22] at a weight ratio of 3 : 1 over the formerly delivered A/G protein. Reaction took place in an antibody incubation solution (Tris-base 50 mM, NaCl 150 mM, pH 8.2) which was shaken at 10°C for 2.5 hours. Finally, the solution went through centrifugation to collect the conjugated quantum dots.

2.4. Instrumental Characterization. Optical properties of nanoparticles were investigated with different spectroscopic measurements such as UV-visible absorption (PB-10 spectrophotometer, Taiwan), photoluminescence (PL, Jobin Yvon Spex Fluorolog 3, Horiba, Japan) of 325 nm excitation wavelength, and Fourier transform infrared spectrometer (FTIR, Tensor 27, Bruker, Germany). The crystal structure and morphology of quantum dots were studied with X-ray diffraction (D8 ADVANCE XRD, Bruker, Germany) taken with an accelerated voltage of 40 kV, a current intensity of 30 mA, a Cu-Kα wavelength of 1.5406 Angstroms, and transmission electron microscopy (TEM, JEM-1400, JEOL, Japan).

3. Results and Discussion

Synthesis temperature, reaction time, and pH values revealed a significant impact on the optical property of CdSe dots. A brief discussion about these influences will be given, and characterization of the best synthesis condition (temperature 100°C, reaction time 4 hours, and pH 11.5) will be provided.

As temperature increased from 90° to 95° and 100°C, UV-visible absorption peaks shifted accordingly (from 470.5 to 489 and 495.5 nm) due to a quantum confinement effect. According to Peng's equation [6], the average sizes of CdSe dots varied from 2.1 nm (90°C) to 2.2 nm (95°C) and 2.3 nm (100°C).

The reaction time effect on particle size distribution was systematically studied (from 1, 2, and 3 to 4 hours). While synthesis temperature was maintained at 100°C, four-hour synthesis exhibited the best absorption and photoluminescent spectra of high, sharp peaks and zero-approaching baselines.

In the CdSe synthesis procedure, Se^{2-} ions were easily oxidized during precursor preparation. To hinder that process, $NaBH_4$ was used to ensure that all SeO_3^{2-} would be transformed into Se^{2-} as described in Dong et al. ([14]):

$$SeO_3^{2-} + BH_4^- \longrightarrow Se^{2-} + B(OH)_3 + H_2O \quad (1)$$

On the other hand, an excessive amount of $NaBH_4$ was easily hydrolyzed as well as oxidized; it then helped create an inert environment and prevent Se^{2-} ions from oxidation.

$$BH_4^- + H_2O \longrightarrow B(OH)_3 + OH^- + H_2 \quad (2)$$

$$BH_4^- + O_2 \longrightarrow B(OH)_3 + H_2O \quad (3)$$

From (1), (2), and (3), it could be expected that a considerable amount of $B(OH)_3$ and OH^- was generated. This vigorously affected the pH value of the solution. To preserve sufficient growth conditions for CdSe quantum dots, pH values had to be adjusted subsequently from 7 to 11.5. Absorption peaks shifted to a longer wavelength when pH values increased. This could be explained by the increase in the dot growth rate when pH values increased in the same synthesis condition including time, temperature, and chemical ratio.

Luminescence intensity was likewise affected as pH values changed. CdSe quantum dot quality presented better improvement in higher pH environments. It could be justified as in higher pH values, thiol groups in MSA could efficiently form more complexes with Cd^{2-} ions. This in turn helped to enhance luminescence intensity by suppressing the surface traps of quantum dots [14, 15, 18].

3.1. Structure Investigation. The X-ray diffraction method was employed to study the structure of CdSe quantum dots (Figure 1). Three typical peaks at 2-theta 25.46°, 44.48°, and 49.91° demonstrated the zincblende structure of CdSe quantum dots, relating to lattice faces of (111), (220), and (311).

Existence of MSA as a capping layer of CdSe quantum dots was successfully validated by two noteworthy signals in FTIR spectra (Figure 2): an absorption band around 1639 cm^{-1} corresponding to vibration bonding C=O in both MSA and CdSe-MSA quantum dots and a peak at around 2571 cm^{-1} relating to S-H bonding, which disappeared in the CdSe-MSA case. These helped confirm MSA-CdSe bonding through the thiol (–SH) groups located on the one side of the acidic molecular structure. With two carboxyl groups facing out, the CdSe-MSA quantum dots were highly ready for further conjugation to functional biogroups. Ultimately, a broad absorption band at around 3303 cm^{-1} of O-H bonding ensured great hydrophilicity of coated CdSe dots.

A transmission electron image of MSA-coated CdSe quantum dots (synthesis temperature 100°C, reaction time 4 hours, and pH 11.5) was taken as shown in Figure 3. Fabricated particles presented a spherical shape with good size homogeneity of approximately 2.3 nm.

We plotted in Figure 4 both the absorption and photoluminescence spectra of a sample optimally synthesized at

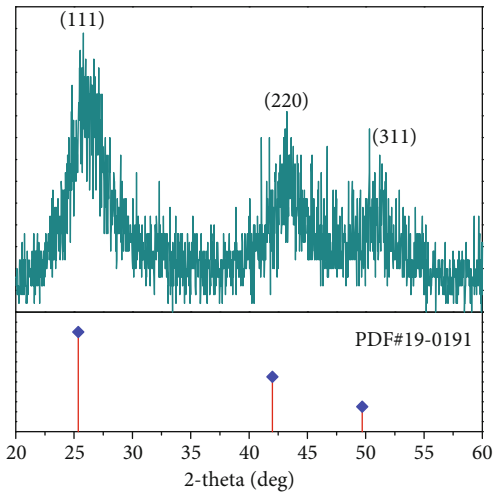

Figure 1: XRD pattern of CdSe quantum dots in a zincblende structure (synthesis temperature 100°C, reaction time 4 hours, and pH 11.5). Three peaks at 25.46°, 44.48°, and 49.9° related to the (111), (220), and (311) lattice direction.

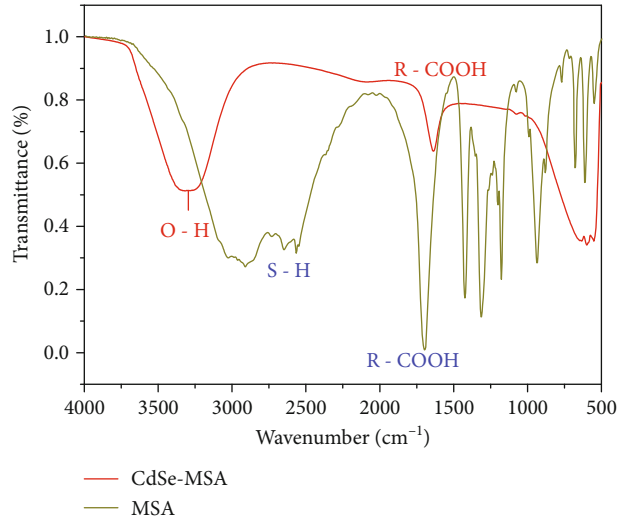

Figure 2: FTIR spectra of MSA (black) and MSA-capped CdSe quantum dots (red).

100°C, pH 11.5, and a reaction time of 4 hours and finally dispersed in PBS 7.0 buffer solution.

The photoluminescence spectrum (red line) presented a high, sharp peak of narrow full width at half maximum. Both sides of the peak approached near zero values. It certified that a 4-hour reaction was optimal for the growth of quantum dots and MSA not only enhanced the luminescence intensity but also helped to passivate surface traps.

A small difference of approximately 0.096 eV existed between absorption and luminescence peaks. Such a tiny deviation verified the high quality of the synthesized quantum dots in which surface traps were inhibited and energy transfer to lattice vibration was limited.

3.2. Toxicity Evaluation of Quantum Dots. According to ISO 10993-5 tests for *in vitro* cytotoxicity, reduction of cell

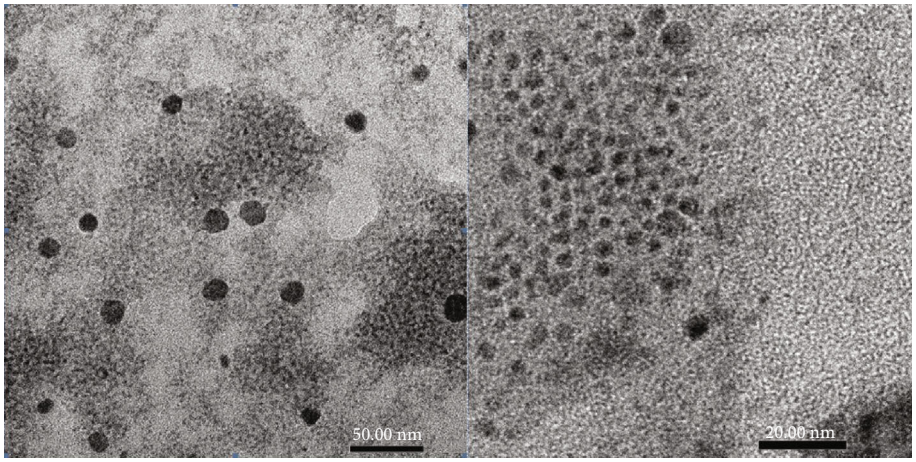

Figure 3: TEM image of MSA-capped CdSe quantum dots at 100°C for 4 h. Uniform sphere-shaped particles of 2.3 nm, in the majority.

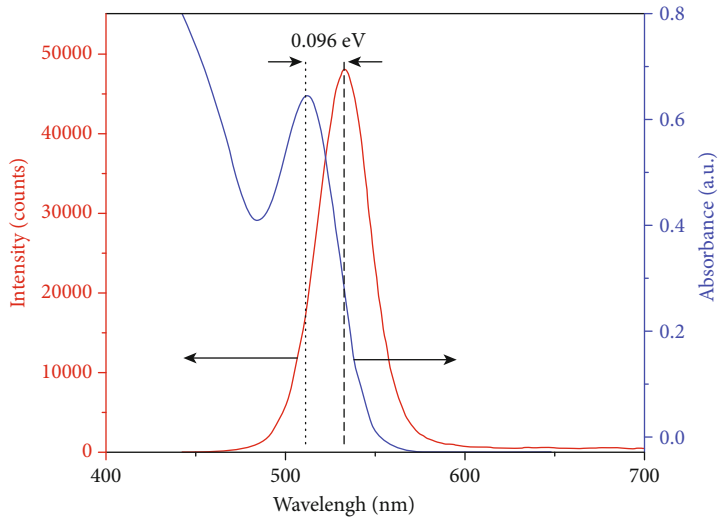

Figure 4: UV-visible absorption (blue) and photoluminescence spectra (red) of CdSe quantum dots optimally synthesized at 100°C, pH 11.5, and a reaction time of 4 hours and dispersed in PBS 7.0 buffer solution.

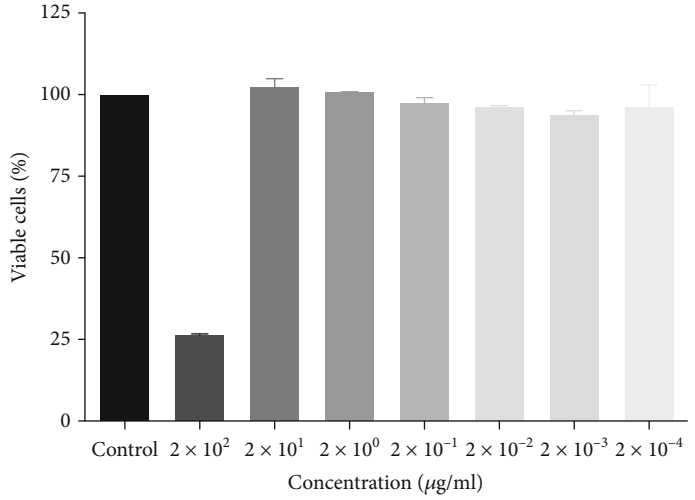

Figure 5: Viability of NIH-3T3 cells exposed to various concentrations of quantum dots. Black-filled bar: naked quantum dots; grey-filled bars: MSA-capped quantum dots.

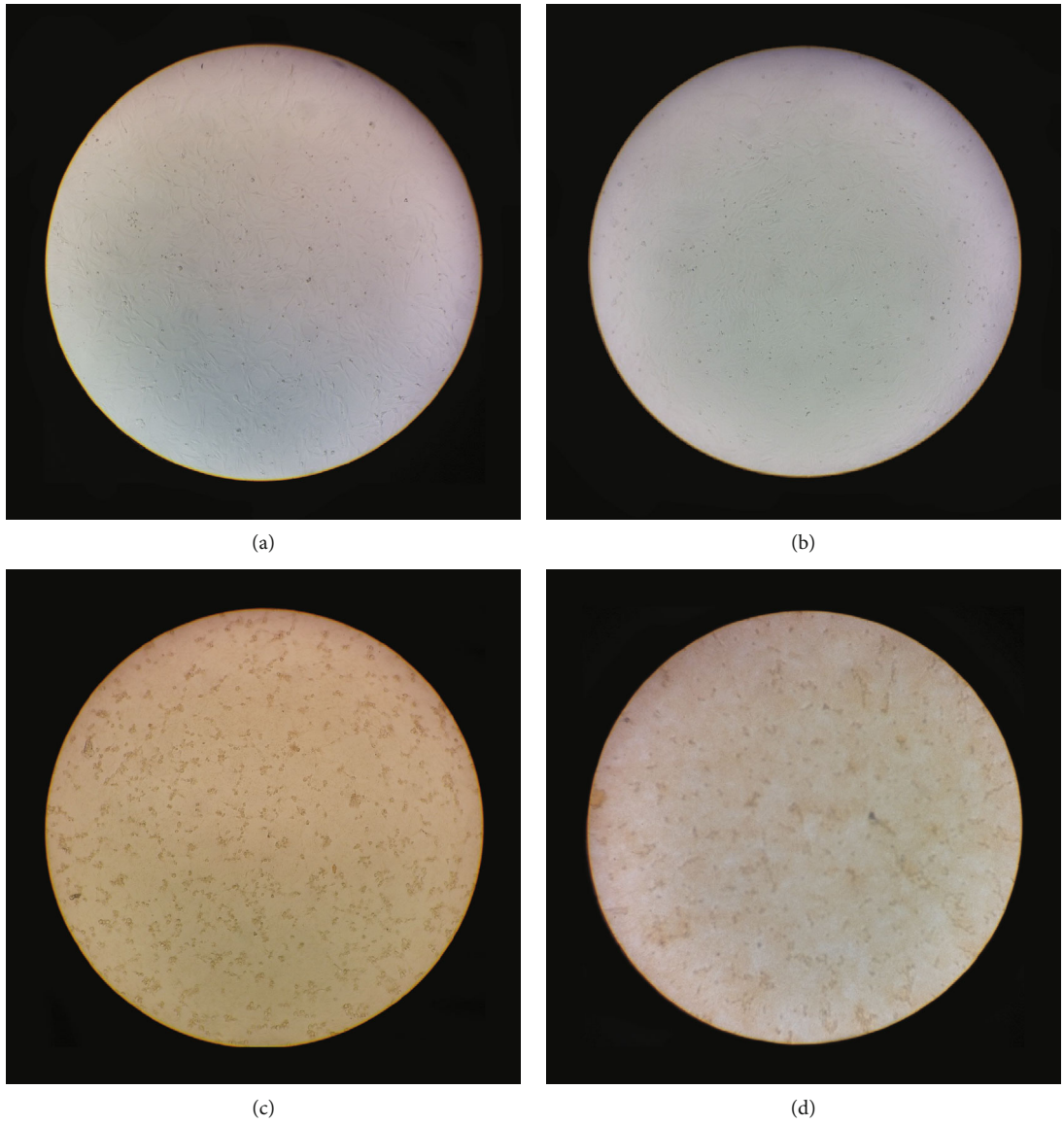

Figure 6: Morphology of NIH-3T3 cells exposed to various quantum dot concentrations: no exposure (a), 20 μg/ml (b), 200 μg/ml (c), and 2000 μg/ml (d).

viability by more than 30% is considered a cytotoxic effect [19]. Figure 5 shows the viability of NIH-3T3 cells exposed to various concentrations of quantum dots.

In accordance with a cytotoxic assay, morphological observation showed the same tendency, as shown in Figure 6. With cells exposed to and incubated in 2×10^2 μg/ml CdSe-MSA or higher, the vitality ratio dropped down to 25.9%, lower than the safety threshold. Cells became smaller and rounder and turned apoptotic. Previous studies show that Cd^{2+} ions are released from the surface of cadmium-based quantum dots. Cadmium is known as a toxic element that induces several adverse effects such as the induction of oxidative stress, mitochondrial dysfunction, apoptosis, and the disruption of intracellular calcium signaling, which leads to their cytotoxic effects [20, 21]. However, there was no obvious morphological change in the presence of quantum dots covered by MSA at the concentrations from 2×10^1 μg/ml to 2×10^{-4} μg/ml; cell vitality ratios remained at a remarkably high level of 97.4% on average. Consequently, at a concentration of 20 μg/ml or less, cells had a great chance for survival. Taken together, we conclude that the highest concentrations of quantum dots that are nontoxic to the NIH-3T3 cell line was at 20 μg/ml.

3.3. Bioconjugation of the CD3 Antibody to MSA-Capped CdSe. Successfully conjugated samples were characterized by photoluminescent and time-resolved fluorescent spectroscopy.

The photoluminescent spectra of MSA-coated CdSe (sample A), A/G protein-MSA-coated CdSe (sample B), and CD3 antibody-A/G protein-MSA-coated CdSe (sample C) are depicted in Figure 7. Interestingly, after connecting with a bridging protein and an antibody, sample

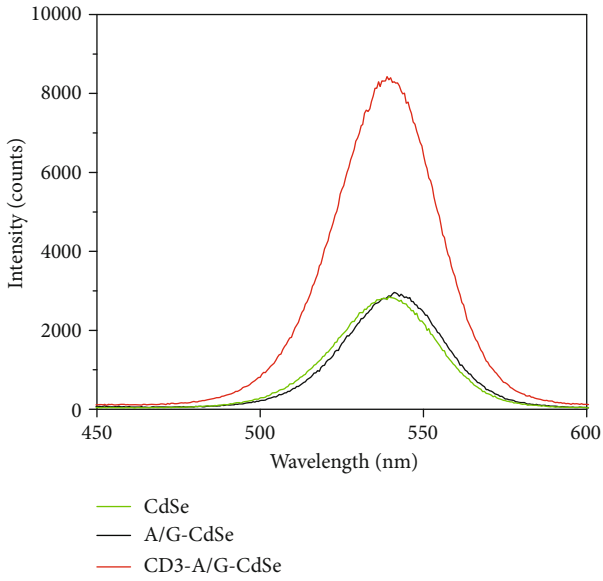

Figure 7: Photoluminescence spectra of MSA-coated CdSe (green), A/G protein-MSA-coated CdSe (black), and CD3 antibody-A/G protein-MSA-coated CdSe (red).

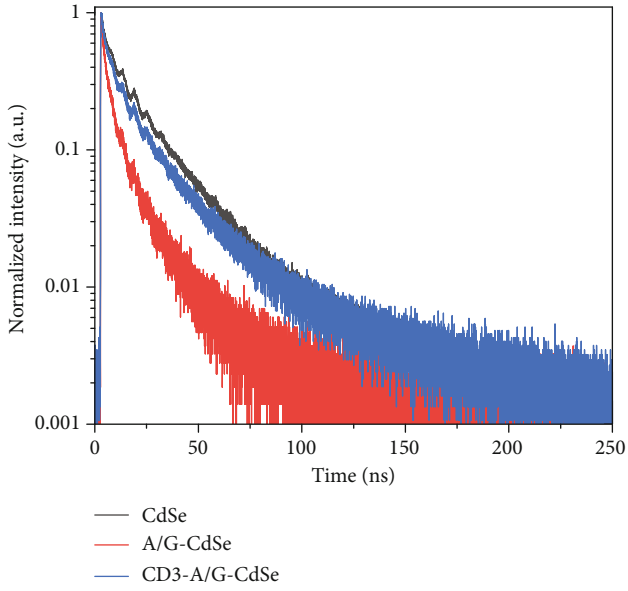

Figure 8: Photoluminescence decay curves of MSA-coated CdSe (black), A/G protein-MSA-coated CdSe (red), and CD3 antibody-A/G protein-MSA-coated CdSe (blue). Excited wavelength of 405 nm.

C exhibited a much higher peak than samples A and B. Such big improvement could probably be explained by lower dangling bonds or traps at the quantum dot surfaces, which might lead to the enhancement of radiative recombination rate and reduction of carrier lifetime. To verify such postulation, the radiative lifetime of the three samples was characterized through time-resolved fluorescence measurements.

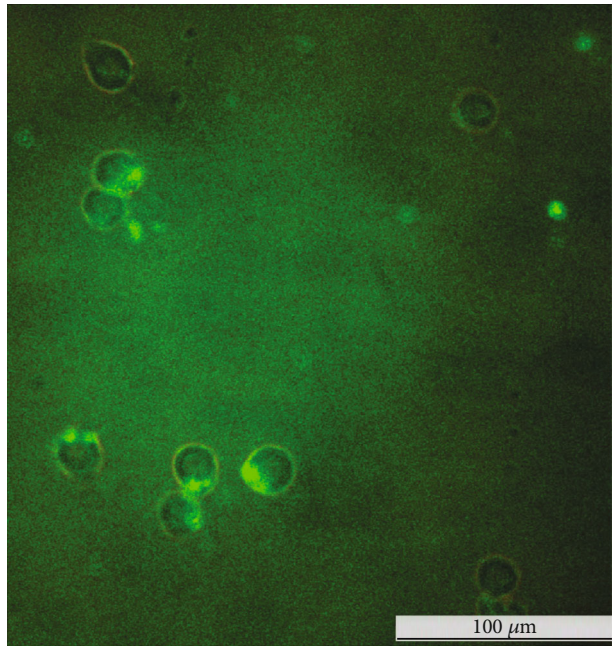

Figure 9: Jurkat T cell labeling evaluation of CD3 antibody-A/G protein-CdSe under fluorescent microscopy.

From time-resolved fluorescence decay curves (Figure 8), the fluorescence lifetime of these samples has been determined by fitting the decay curves with a triexponential function:

$$I(t) = A_1 \cdot \exp\left(-\frac{t}{\tau_1}\right) + A_2 \cdot \exp\left(-\frac{t}{\tau_2}\right) + A_3 \cdot \exp\left(-\frac{t}{\tau_3}\right), \quad (4)$$

where τ_1, τ_2, and τ_3 are the first, second, and third components of lifetimes and A_1, A_2, and A_3 are the corresponding relative weights of these components. The average fluorescence lifetimes for the decay curves were calculated from the decay times and the relative contribution of the components using the following equation:

$$\tau_{av} = \tau_1.A_1 + \tau_2.A_2 + \tau_3.A_3 \quad (5)$$

The fluorescence showed a triexponential decay with average lifetimes of 11.9, 11.9, and 9.1 nanoseconds for MSA-coated CdSe, A/G protein-MSA-coated CdSe, and CD3 antibody-A/G protein-MSA-coated CdSe, respectively.

A shorter radiative lifetime and low nonradiative recombination of carriers in sample C also helped to explain the strong luminescence compared with samples A and B (Figure 7). This is quite convenient and suitable for time-saving detection under fluorescent microscopy.

3.4. Jurkat T Cell Labeling Assessment. In addition to other spectroscopic or microscopic methods, confocal laser scanning microscopy has been considered an effective tool to verify the conjugation of bioagents on quantum dots [8, 10] and

the successful applications of nanoparticles in the biomedical field [9, 23–26].

To evaluate cell detection capability, CD3-A/G-CdSe was mixed at a volume ratio of 1 : 3 with Jurkat T cells preserved in RPMI 1640 solution. The mixture was delivered into several microcentrifuge tubes and moderately shaken for 30 minutes. Thereafter, those tubes went through centrifugation of 1500 rounds per minute for 5 minutes to eliminate unnecessary supernatants. The final product was characterized by fluorescent microscopy as shown in Figure 9. High fluorescent intensity could be observed on the membrane of Jurkat T cells where the quantum dots were located. This led to two solid conclusions: (1) good coupling between CD3 antibody-A/G protein-CdSe and cell antigen and (2) substantial bonding between quantum dots and cells.

4. Conclusion

In summary, we successfully synthesized MSA-coated CdSe by a simple green method at low temperature with cost-saving chemicals. The influence of reaction time, temperature, and pH values on optical property was spectroscopically characterized. Uniformly distributed 2.3 nm acid-coated quantum dots of high quality, high luminescence, and high biocompatibility were produced at 100°C, a pH value of 11.5, and a four-hour reaction. The toxicity of MSA-capped CdSe quantum dots was evaluated using the NIH-3T3 cell line (ATCC® CRL-1658™) and the MTT assay resulting in a secure threshold of 20 μg/ml. The CD3 antibody was successfully conjugated to the MSA-capped CdSe with the assistance of the A/G protein. Photoluminescence and time-resolved fluorescence were employed for verification. Lifetimes were found to decrease from 11.9 nanoseconds for MSA-coated CdSe and A/G protein-MSA-coated CdSe down to 9.1 ns for the CD3 antibody-A/G protein-MSA-coated CdSe, respectively. The final conjugated CdSe quantum dots were mixed with Jurkat T cells to evaluate detection ability. Fluorescent microscopic results evidently exhibited great coupling of the CD3 antibody and antigens and validated the high possibility of CdSe-based biosensors. The achieved products are ready for the coming steps of development.

Data Availability

The data used to support the findings of this study are included within the article and available from the corresponding authors upon request.

Conflicts of Interest

The authors declare that they have no conflict of interest.

Acknowledgments

This work was supported by the Priming Scientific Research Foundation and the Department of Science and Technology of Ho Chi Minh City (Project no. 105/2017/HD-SKHCN).

References

[1] V. Biju, T. Itoh, and M. Ishikawa, "Delivering quantum dots to cells: bioconjugated quantum dots for targeted and nonspecific extracellular and intracellular imaging," *Chemical Society Reviews*, vol. 39, no. 8, pp. 3031–3056, 2010.

[2] J. F. Callan and R. C. Mulrooney, "Luminescent detection of Cu(II) ions in aqueous solution using CdSe and CdSe-ZnS quantum dots functionalised with mercaptosuccinic acid," *physica status solidi (c)*, vol. 6, no. 4, pp. 920–923, 2009.

[3] S. Chen, X. Zhang, Q. Zhang et al., "CdSe quantum dots decorated by mercaptosuccinic acid as fluorescence probe for Cu^{2+}," *Journal of Luminescence*, vol. 131, no. 5, pp. 947–951, 2011.

[4] W. E. Mahmoud, "Functionalized ME-capped CdSe quantum dots based luminescence probe for detection of Ba^{2+} ions," *Sensors and Actuators B: Chemical*, vol. 164, no. 1, pp. 76–81, 2012.

[5] Z. Zhelev, H. Ohba, R. Bakalova et al., "Fabrication of quantum dot–lectin conjugates as novel fluorescent probes for microscopic and flow cytometric identification of leukemia cells from normal lymphocytes," *Chemical Communications*, vol. 15, no. 15, pp. 1980–1982, 2005.

[6] C. Cai, H. Cheng, Y. Wang, and H. Bao, "Mercaptosuccinic acid modified CdTe quantum dots as a selective fluorescence sensor for A^{g+}determination in aqueous solutions," *RSC Advances*, vol. 4, no. 103, pp. 59157–59163, 2014.

[7] M. S. Hosseini and A. Pirouz, "Study of fluorescence quenching of mercaptosuccinic acid-capped CdS quantum dots in the presence of some heavy metal ions and its application to Hg(II) ion determination," *Luminescence*, vol. 29, no. 7, pp. 798–804, 2014.

[8] S. Dwarakanath, J. G. Bruno, A. Shastry et al., "Quantum dot-antibody and aptamer conjugates shift fluorescence upon binding bacteria," *Biochemical and Biophysical Research Communications*, vol. 325, no. 3, pp. 739–743, 2004.

[9] G. Giraud, H. Schulze, T. Bachmann et al., "Fluorescence lifetime Imaging of Quantum dot labeled DNA microarrays," *International Journal of Molecular Sciences*, vol. 10, no. 4, pp. 1930–1941, 2009.

[10] H. Udaka, T. Fukuda, N. Kamata, and M. Suzuki, "Evaluation of CdSe/ZnS quantum dot–half anti CD3 antibody–conjugate using confocal laser scanning microscopy," *Molecular Crystals and Liquid Crystals*, vol. 653, no. 1, pp. 177–181, 2017.

[11] S. A. Rahman, N. Ariffin, N. A. Yusof et al., "Synthesis and surface modification of biocompatible water soluble core-shell quantum dots," *Advanced Materials Research*, vol. 879, pp. 184–190, 2014.

[12] S. Rosenthal, J. Mcbride, S. Pennycook, and L. Feldman, "Synthesis, surface studies, composition and structural characterization of CdSe, core/shell and biologically active nanocrystals," *Surface Science Reports*, vol. 62, no. 4, pp. 111–157, 2007.

[13] R. A. Sperling and W. J. Parak, "Surface modification, functionalization and bioconjugation of colloidal inorganic nanoparticles," *Philosophical Transactions of the Royal Society A: Mathematical, Physical and Engineering Sciences*, vol. 368, no. 1915, pp. 1333–1383, 2010.

[14] M. Dong, J. Xu, S. Liu, Y. Zhou, and C. Huang, "Synthesis of highly luminescent mercaptosuccinic acid-coated CdSe nanocrystals under atmospheric conditions," *Luminescence*, vol. 29, no. 7, pp. 818–823, 2014.

[15] S. Li, H. Zhao, and D. Tian, "Aqueous synthesis of highly monodispersed thiol-capped CdSe quantum dots based on the electrochemical method," *Materials Science in Semiconductor Processing*, vol. 16, no. 1, pp. 149–153, 2013.

[16] J. T. Siy, E. M. Brauser, and M. H. Bartl, "Low-temperature synthesis of CdSe nanocrystal quantum dots," *Chemical Communications*, vol. 47, no. 1, pp. 364–366, 2011.

[17] Y. Wang, S. Liu, H. Pan, K. Yang, and L. Zhou, "Synthesis of high-quality CdSe quantum dots in aqueous solution," *Micro & Nano Letters*, vol. 7, no. 9, pp. 889–891, 2012.

[18] E. Ying, D. Li, S. Guo, S. Dong, and J. Wang, "Synthesis and bio-imaging application of highly luminescent mercaptosuccinic acid-coated CdTe nanocrystals," *PLoS One*, vol. 3, no. 5, p. e2222, 2008.

[19] ISO, "ISO 10993-5:2009 Biological evaluation of medical devices—part 5: tests for in vitro cytotoxicity," 2009, https://www.iso.org/standard/36406.html.

[20] C. Kirchner, T. Liedl, S. Kudera et al., "Cytotoxicity of colloidal CdSe and CdSe/ZnS nanoparticles," *Nano Letters*, vol. 5, no. 2, pp. 331–338, 2005.

[21] L. Peng, M. He, B. Chen et al., "Cellular uptake, elimination and toxicity of CdSe/ZnS quantum dots in HepG2 cells," *Biomaterials*, vol. 34, no. 37, pp. 9545–9558, 2013.

[22] P. Humeniuk, S. Geiselhart, C. Battin et al., "Generation of a Jurkat-based fluorescent reporter cell line to evaluate lipid antigen interaction with the human INKT cell receptor," *Scientific Reports*, vol. 9, no. 1, p. 7426, 2019.

[23] B. H. Lee, S. Suresh, and A. Ekpenyong, "Fluorescence intensity modulation of CdSe/ZnS quantum dots assesses reactive oxygen species during chemotherapy and radiotherapy for cancer cells," *Journal of Biophotonics*, vol. 12, no. 2, p. e201800172, 2018.

[24] M. Röding, S. J. Bradley, M. Nydén, and T. Nann, "Fluorescence lifetime analysis of graphene quantum dots," *The Journal of Physical Chemistry C*, vol. 118, no. 51, pp. 30282–30290, 2014.

[25] B. Zhang, C. Yang, Y. Gao et al., "Mechanisms of fluorescence decays of colloidal CdSe–CdS/ZnS quantum dots unraveled by time-resolved fluorescence measurement," *Physical Chemistry Chemical Physics*, vol. 17, no. 41, pp. 27588–27595, 2015.

[26] B. Zhang, C. Yang, Y. Gao et al., "Engineering quantum dots with different emission wavelengths and specific fluorescence lifetimes for spectrally and temporally multiplexed imaging of cells," *Nanotheranostics*, vol. 1, no. 1, pp. 131–140, 2017.